

FREE VIBRATION OF COMPOSITE CYLINDRICAL SHELLS WITH ORTHOGONAL STIFFENERS

YONGFU WU, CHEN ZHAO, HAOFENG LIANG, SISHI YAO, JIANGHONG XUE, PENG XU
*Key Lab of Disaster Forecast and Control in Engineering, Ministry of Education,
School of Mechanics and Construction Engineering, Jinan University, Guangzhou, China
e-mail: txuej@jnu.edu.cn (Jianghong Xue); xupeng@stu2019.jnu.edu.cn (Peng Xu)*

This paper proposes theoretical and numerical approaches to scrutinize the free vibration of orthogonal stiffened cylindrical shells. According to Kármán-Donnell shell theory, the total energy of the stiffened cylindrical shells is derived. Based on the principle of minimum potential energy, the eigenfunction related to the frequency is established and solved by developing a MATLAB program. Analytical solutions of the natural frequency for free vibration of the stiffened cylindrical shells are calculated and are verified against the finite element results from ABAQUS software. On account of the observations from the parametric study, an optimization scheme of the stiffeners is proposed.

Keywords: free vibration, laminated cylindrical shell, stiffener, energy method

1. Introduction

With the development of industry and economy, cylindrical shell structures are widely used in many fields including civil engineering, marine industry and aerospace engineering. In practical engineering, cylindrical shell structures are usually subjected to various loads. Because of the importance of cylindrical shells in engineering, theoretical and experimental studies have been conducted.

Li *et al.* (2013) detailed calculating formulas about deformation and stress of large diameter cylindrical shells with the cross-section obtained by programming, which can be used in storage tank design such as petroleum reserve. Xue *et al.* (2015) proposed a first order shear deformation theory for cylindrical sandwich pipes subjected to undersea water pressure. Schneider and Zahlten (2004) conducted physically and geometrically nonlinear analyses of the load-bearing capacity of slender wind-loaded cylindrical shells and drew some conclusions for the design practice from nonlinear parameter studies. Based on Kármán-Donnell's theory, Xue (2012, 2013) and Xue *et al.* (2013) presented a unique approach to analyze the buckling of an infinitely long cylindrical shell and the post-buckling of a pipe subjected to external pressure. As to the structural failure, such as buckling and postbuckling, stiffened cylindrical shells were examined by Bisagni and Cordisco (2006) using an experimental approach, by Wang *et al.* (2007) to explore the characteristics and regularity of ring-stiffened cylindrical shells under different cross uniform external pressures and by Sadeghifar *et al.* (2010) to employ a genetic algorithm and energy discrete calculation method for axial buckling optimization of orthogonally stiffened cylindrical shells. The influence of initial geometric imperfections in the shapes of eigenmodes and periodic modes on the load-carrying capacity of a steel stringer-stiffened cylindrical shell subject to axial compression was studied by Sadovský *et al.* (2009).

Vibration characteristics of shell structures have been one of the research focuses of scholars worldwide. Mohamad (2002) and Mohamad *et al.* (2010) summarized the research on dynamic studies of the shell structures. Breslavskii *et al.* (2011) proposed a method to calculate nonlinear

vibrations of shallow shells in fluid, then expanded the nonlinear vibrations of a shell in terms of the normal modes of the system. Swamy Naidu and Sinha (2007) investigated nonlinear free vibration behavior of laminated composite shells subjected to hydrothermal environments using the finite element method and carried out a parametric study of variable curvature ratios and side to thickness ratios of composite cylindrical shells. Lee and Kwak (2015) used the Rayleigh-Ritz method to derive a dynamic model for free vibration analysis of a circular cylindrical shell and established explicit expressions for the mass and stiffness matrices.

Some studies are presently available for vibration of stiffened cylindrical shells. The analysis of free vibration of rotating functionally graded carbon nanotube reinforced composite cylindrical shells with arbitrary boundary conditions was inspected by Qin *et al.* (2019). Both Hemmatnezhad *et al.* (2015) and Jafari and Bagheri (2006) investigated in detail the free vibration problem of stiffened composite cylindrical shells from three aspects of theory, experiment and numerical simulation. Besides, Li *et al.* (2015) researched the free vibration response of joined and orthogonally stiffened cylindrical-spherical shells and explored the effects of the crucial factor by the finite element software ANSYS. Rout *et al.* (2017) analyzed free vibration of delaminated composite stiffened shallow shells employing the finite element method. Based on the Flügge thin shell theory and Hamilton principle, Zhou (2012) addressed the fluid-solid coupling vibration of a circumferential stiffened cylindrical shell filled with a liquid. In addition, the free vibration of circumferential stiffened cylindrical shells was also studied by means of wave propagation, see Gan *et al.* (2009), by the Galerkin method, see Ahmadi and Foroutan (2019). As to the nonlinear vibration of the stiffened cylindrical shells, Torkamani *et al.* (2009) built a free vibration model of a longitudinal and transverse ribbed cylindrical shell based on the nonlinear stress-strain relationship in the Kármán-Donnell shell theory. The natural frequency of the shell was solved using the principle of virtual work. Using von Kármán nonlinear thin shell theory and first-order shear theory, Sheng and Wang (2018) analyzed dynamic stability and nonlinear vibration of functionally graded material stiffened cylindrical shells by the uniform distribution of the stiffness method.

The above studies on dynamic responses of the stiffened cylindrical shells are accomplished by analyzing the deformation kinematics of the stiffeners and the cylindrical shells separately. Due to the undetermined contact forces between the stiffeners and the cylindrical shell, it is different to simultaneously solve the differential equations of equilibrium of the stiffeners and the cylindrical shell, especially when the number of stiffeners is large. In the present study, the energy method is proposed to analyze the free vibration of the reinforced cylindrical shells with which the coupled differential equations of equilibrium of the stiffeners and the cylindrical shell are unnecessary to solve. Strain and kinetic energy of the cylindrical shell and stiffeners undergoing free vibration are derived based on the Kármán-Donnell shell theory and are calculated by developing a MATLAB program. The finite element models for cylindrical shells with stiffeners in circumferential and longitudinal directions are established in ABAQUS software. The numerical solutions are compared with the theoretical solutions to validate the feasibility of the energy method. With the established energy method, the effects of number of the stiffeners, geometric parameters and material properties of stiffeners on the free vibration of the stiffened cylindrical shells are discussed, and the optimization of the reinforcement scheme is proposed.

2. Fundamental formulas

Figure 1 illustrates a simply supported laminated cylindrical shell with orthogonal stiffeners in the circumferential and axial directions. The stiffened cylindrical shell is decomposed into three components: a laminated cylindrical shell, circumferential ribs and longitudinal ribs. The cylindrical shell has a length of L , a radius of R and a thickness of h . The circumferential ribs

are circular rings of width b_c , thickness h_c and radius $R - h_c/2$, and the longitudinal ribs are rectangular bars with a width of b_l , a thickness of h_l and a length of L . A coordinate system is located at the middle surface of the laminated cylindrical shell where x , y and z represent the axial, circumferential and radial directions, respectively.

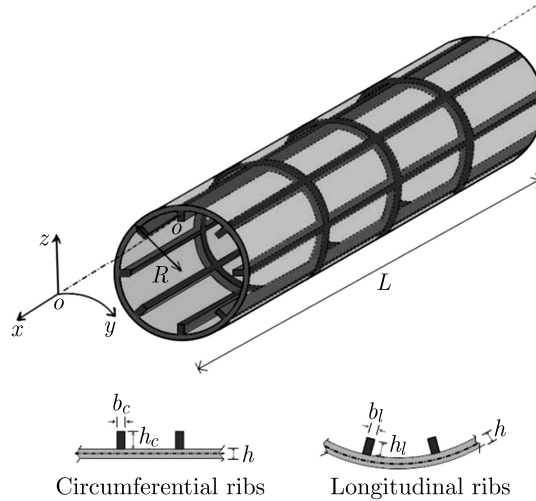


Fig. 1. Coordinate system and an orthogonally stiffened cylindrical shell

2.1. Deformation kinematics

Define u , v and w as the components of the displacement of the stiffened laminated cylindrical shell in the axial, circumferential and radial directions. According to Kármán-Donnell's shell theory, the components of strain ε_{ij} and the changes of curvature κ_{ij} of the stiffened shell are expressed as

$$\varepsilon_x = u_{,x} \quad \varepsilon_y = v_{,y} + \frac{w}{R} \quad \gamma_{xy} = u_{,y} + v_{,x} \quad (2.1)$$

and

$$\kappa_x = -w_{,xx} \quad \kappa_y = -w_{,yy} \quad \kappa_{xy} = -w_{,xy} \quad (2.2)$$

Xue *et al.* (2013) have shown that for a non-shallow cylindrical shell with the initial curvature of $1/R$, the deflection in the radial direction w will cause an extra change in curvature κ_y by an amount of $-w/R^2$. Thus, the total change of curvature in the circumferential direction is modified to

$$\kappa'_y = -w_{,yy} - \frac{w}{R^2} \quad (2.3)$$

It is often assumed in theories of beams, plates and shells that the components of strain and the changes of curvature are invariable along the thickness of the structures, and the deformation is characterized by the component of displacement of the neutral surface. Suppose that the i -th circumferential rib is located at $x = x_i$ on the cylindrical shell and the j -th longitudinal rib is at $y = y_j$ on the cylindrical shell. Thus, due to the continuity conditions between the laminated cylindrical shell and the ribs, the components of displacement of the circumferential ribs and of the longitudinal ribs are the same as those of the cylindrical shell at the corresponding places, i.e.

$$\begin{aligned} u_i^c &= u|_{x=x_i} & v_i^c &= v|_{x=x_i} & w_i^c &= w|_{x=x_i} & \text{for } i &= 1, \dots, r \\ u_j^l &= u|_{y=y_j} & v_j^l &= v|_{y=y_j} & w_j^l &= w|_{y=y_j} & \text{for } j &= 1, \dots, s \end{aligned} \quad (2.4)$$

where u_i^c , v_i^c and w_i^c are the components of displacement of the i -th circumferential rib, u_j^l , v_j^l and w_j^l are the components of displacement of the j -th longitudinal rib, r is the number of circumferential rib and s the number of longitudinal rib.

Similarly, the components of strain and the changes of curvature in the circumferential and longitudinal ribs are the same as those of the cylindrical shell, i.e.:

— for circumferential ribs

$$\varepsilon_i^c = \varepsilon_y|_{x=x_i} = v_{i,y}^c + \frac{1}{R}w_i^c \quad \kappa_i^c = \kappa'_y|_{x=x_i} = -w_{i,yy}^c - \frac{1}{R^2}w_i^c \quad (2.5)$$

— for longitudinal ribs

$$\varepsilon_j^l = \varepsilon_x|_{y=y_j} = u_{j,x}^l \quad \kappa_j^l = \kappa_x|_{y=y_j} = -w_{j,xx}^l \quad (2.6)$$

2.2. Constitutive relations

As indicated in Section 2, the stiffened cylindrical shell is composed of the cylindrical shell, circumferential ribs and longitudinal ribs. For a general purpose, the cylindrical shell is considered to be made of composite laminates, while the circumferential and the longitudinal ribs are manufactured of isotropic materials.

2.2.1. Laminated cylindrical shell

The material properties of the composite ply for the cylindrical shell are E_{11} , E_{22} , μ_{12} , μ_{21} , G_{12} which represent Young's modulus in the first and second principal direction, Poisson's ratio in the corresponding direction and the shear modulus of the composite ply, respectively. Suppose that the angle of the orientation of the k -th ply with respect to the horizontal axis in the global coordinate systems for the cylindrical shell is θ . The stiffness matrix $\overline{\mathbf{Q}}_k$ of the k -th composite ply in the global coordinate system of the cylindrical shell are formulated as follows

$$\overline{\mathbf{Q}}_k = \begin{bmatrix} (\overline{Q}_{11})_k \\ (\overline{Q}_{12})_k \\ (\overline{Q}_{22})_k \\ (\overline{Q}_{16})_k \\ (\overline{Q}_{26})_k \\ (\overline{Q}_{66})_k \end{bmatrix} = \begin{bmatrix} c^4 & 2c^2s^2 & s^4 & 4c^2s^2 \\ c^2s^2 & c^4 + s^4 & c^2s^2 & -4c^2s^2 \\ s^4 & 2c^2s^2 & c^4 & 4c^2s^2 \\ c^3s & cs^3 - c^3s & -cs^3 & -2cs(c^2 - s^2) \\ cs^3 & c^3s - cs^3 & -c^3s & 2cs(c^2 - s^2) \\ c^2s^2 & -2c^2s^2 & c^2s^2 & (c^2 - s^2)^2 \end{bmatrix} \begin{bmatrix} Q_{11} \\ Q_{12} \\ Q_{22} \\ Q_{66} \end{bmatrix} \quad (2.7)$$

where $c = \cos \theta$, $s = \sin \theta$ and

$$\begin{aligned} Q_{11} &= \frac{E_{11}}{1 - \mu_{12}^{(1)}\mu_{21}^{(1)}} & Q_{22} &= \frac{E_{22}}{1 - \mu_{12}^{(1)}\mu_{21}^{(1)}} \\ Q_{12} &= \frac{\mu_{21}E_{22}}{1 - \mu_{12}^{(1)}\mu_{21}^{(1)}} = \frac{\mu_{12}E_{11}}{1 - \mu_{12}^{(1)}\mu_{21}^{(1)}} & Q_{66} &= G_{12} \end{aligned} \quad (2.8)$$

The matrix of tensile stiffness \mathbf{A} , coupling stiffness \mathbf{B} and bending stiffness \mathbf{D} for the cylindrical shell are computed by

$$A_{pq} = \int_{-h/2}^{h/2} (\overline{Q}_{pq})_k dz \quad B_{pq} = \int_{-h/2}^{h/2} (\overline{Q}_{pq})_k z dz \quad D_{pq} = \int_{-h/2}^{h/2} (\overline{Q}_{pq})_k z^2 dz \quad (2.9)$$

where k is the layer number of the composite ply of the cylindrical shell. According to mechanics of composite materials, the constitutive relationships for laminated cylindrical shells are

expressed as

$$\begin{bmatrix} N_x \\ N_y \\ N_{xy} \\ M_x \\ M_y \\ M_{xy} \end{bmatrix} = \begin{bmatrix} A_{11} & A_{12} & A_{16} & B_{11} & B_{12} & B_{16} \\ A_{12} & A_{22} & A_{26} & B_{12} & B_{22} & B_{26} \\ A_{16} & A_{26} & A_{66} & B_{16} & B_{26} & B_{66} \\ B_{11} & B_{12} & B_{16} & D_{11} & D_{12} & D_{16} \\ B_{12} & B_{22} & B_{26} & D_{12} & D_{22} & D_{26} \\ B_{16} & B_{26} & B_{66} & D_{16} & D_{26} & D_{66} \end{bmatrix} \begin{bmatrix} \varepsilon_x \\ \varepsilon_y \\ \gamma_{xy} \\ \kappa_x \\ \kappa_y \\ \kappa_{xy} \end{bmatrix} \quad (2.10)$$

where N_{ij} and M_{ij} are the membrane forces and bending moments of the laminated cylindrical shell, respectively.

2.2.2. Stiffening ribs

When the ribs vibrate with the shell, the bending stiffness EI of an independent rib is no longer applicable in this case. As the stiffening ribs are mounted on the cylindrical shell, there exists an interaction between the cylindrical shell and the ribs which cause extra stiffness of the cylindrical shell and the ribs. To avoid solving the complex interaction between the cylindrical shell, portions of the cylindrical shell that are connected with the ribs are taken out and are added to the ribs to form integrated stiffeners. The integrated stiffeners in the longitudinal and circumferential direction have geometry sizes of $L \times b_c \times (h_c + h)$ and $2\pi R \times b_l \times (h_l + h)$.

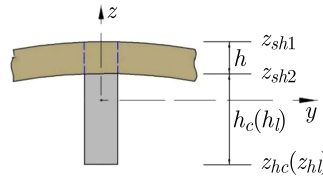


Fig. 2. Model of coupling vibration between the stiffeners and laminated cylindrical shell

Figure 2 illustrates geometry of the integrated stiffeners as well as their neutral axis. According to the mechanics of composite materials, the membrane stiffness \mathbf{A} , the tension-bending coupling stiffness \mathbf{B} and the bending stiffness \mathbf{D} of the integrated stiffeners are calculated as follows

$$\begin{aligned} A_{11}^{(c)} &= \int_{z_{sh2}}^{z_{sh1}} (\bar{Q}_{pq})_k dz + \int_{z_{hc}}^{z_{sh2}} Q_{11}^{(c)} dz & A_{11}^{(l)} &= \int_{z_{sh2}}^{z_{sh1}} (\bar{Q}_{pq})_k dz + \int_{z_{hl}}^{z_{sh2}} Q_{11}^{(l)} dz \\ B_{11}^{(c)} &= \int_{z_{sh2}}^{z_{sh1}} (\bar{Q}_{pq})_k z dz + \int_{z_{hc}}^{z_{sh2}} Q_{11}^{(c)} z dz & B_{11}^{(l)} &= \int_{z_{sh2}}^{z_{sh1}} (\bar{Q}_{pq})_k z dz + \int_{z_{hl}}^{z_{sh2}} Q_{11}^{(l)} z dz \\ D_{11}^{(c)} &= \int_{z_{sh2}}^{z_{sh1}} (\bar{Q}_{pq})_k z^2 dz + \int_{z_{hc}}^{z_{sh2}} Q_{11}^{(c)} z^2 dz & D_{11}^{(l)} &= \int_{z_{sh2}}^{z_{sh1}} (\bar{Q}_{pq})_k z^2 dz + \int_{z_{hl}}^{z_{sh2}} Q_{11}^{(l)} z^2 dz \end{aligned} \quad (2.11)$$

where $z_{sh1} = (h + h_c(h_l))/2$, $z_{sh2} = (-h + h_c(h_l))/2$, $z_{hc} = -(h + h_c)/2$, $z_{hl} = -(h + h_l)/2$, Q_{11} and Q_{22} represent the reduced stiffness coefficient of the cylindrical shell in the longitudinal and circumferential direction, respectively, the superscripts (c) and (l) of \mathbf{A} , \mathbf{B} and \mathbf{D} refer to the integrated stiffeners in the circumferential and longitudinal direction, respectively, $Q_{11}^{(c)}$ and $Q_{11}^{(l)}$ represent the reduced stiffness coefficient of the circumferential and longitudinal ribs, respectively, and are calculated as follows

$$Q_{11}^{(c)} = \frac{E_c}{1 - \mu_c^2} \quad Q_{11}^{(l)} = \frac{E_l}{1 - \mu_l^2} \quad (2.12)$$

where E_c , E_l and μ_x , μ_y represent the elastic modulus and Poisson's ratio of the circumferential and longitudinal ribs, respectively.

The constitutive relationships for the circumferential stiffeners and longitudinal stiffeners are simplified as

$$\begin{bmatrix} N_c \\ M_c \end{bmatrix} = \begin{bmatrix} A_{11}^{(c)} & B_{11}^{(c)} \\ B_{11}^{(c)} & D_{11}^{(c)} \end{bmatrix} \begin{bmatrix} \varepsilon_c \\ \kappa_c \end{bmatrix} \quad \begin{bmatrix} N_l \\ M_l \end{bmatrix} = \begin{bmatrix} A_{11}^{(l)} & B_{11}^{(l)} \\ B_{11}^{(l)} & D_{11}^{(l)} \end{bmatrix} \begin{bmatrix} \varepsilon_l \\ \kappa_l \end{bmatrix} \quad (2.13)$$

where N_c , N_l and M_c , M_l are the membrane forces and bending moments of the circumferential and longitudinal stiffeners, respectively.

3. Free vibration of stiffened cylindrical shells

During vibration of the stiffened cylindrical shell, the energy dissipates in the form of strain energy and kinetic energy. The strain energy U and kinetic energy T of the stiffened cylindrical shell are summation of the corresponding energy dissipated by the cylindrical shell, the circumferential and longitudinal stiffeners as follows

$$U = U_{shell} + U_c + U_l \quad T = T_{shell} + T_c + T_l \quad (3.1)$$

where U_{shell} , U_c and U_l is the strain energy dissipated by the cylindrical shell, the circumferential and longitudinal stiffeners, respectively. T_{shell} , T_c and T_l is the kinetic energy dissipated by the cylindrical shell, the circumferential and longitudinal stiffeners, respectively. They are given by

$$\begin{aligned} U_{shell} &= \frac{1}{2} \iint (M_x \kappa_x + M_y \kappa_y + 2M_{xy} \kappa_{xy}) dx dy + \frac{1}{2} \iint (N_x \varepsilon_x + N_y \varepsilon_y + 2N_{xy} \varepsilon_{xy}) dx dy \\ &= \frac{1}{2} \int_0^L \int_0^{2\pi R} (D_{11} \kappa_x \kappa_x + 2D_{12} \kappa_x \kappa_y + D_{22} \kappa_y \kappa_y + 4D_{66} \kappa_{xy} \kappa_{xy} \\ &\quad + A_{11} \varepsilon_x \varepsilon_x + 2A_{12} \varepsilon_x \varepsilon_y + A_{22} \varepsilon_y \varepsilon_y + A_{66} \gamma_{xy} \gamma_{xy}) dx dy \end{aligned} \quad (3.2)$$

$$U_c = \sum_{i=0}^{n_i} \frac{1}{2} b_c \int_0^{2\pi R} (A_{11}^{(c)} \varepsilon_i^c \varepsilon_i^c + 2B_{11}^{(c)} \varepsilon_i^c \kappa_i^c + D_{11}^{(c)} \kappa_i^c \kappa_i^c) \Big|_{x=c_i} dy$$

$$U_l = \sum_{j=0}^{n_j} \frac{1}{2} b_l \int_0^L (A_{11}^{(l)} \varepsilon_j^l \varepsilon_j^l + 2B_{11}^{(l)} \varepsilon_j^l \kappa_j^l + D_{11}^{(l)} \kappa_j^l \kappa_j^l) \Big|_{y=d_j} dx$$

and

$$\begin{aligned} T_{shell} &= \frac{1}{2} \rho h \int_0^L \int_0^{2\pi R} [(\dot{u})^2 + (\dot{v})^2 + (\dot{w})^2] dx dy \\ T_c &= \sum_{i=0}^{n_i} \frac{1}{2} \rho_c b_c h_c \int_0^{2\pi R} [(\dot{u}_i^c)^2 + (\dot{v}_i^c)^2 + (\dot{w}_i^c)^2] \Big|_{x=c_i} dy \\ T_l &= \sum_{j=0}^{n_j} \frac{1}{2} \rho_l b_l h_l \int_0^L [(\dot{u}_j^l)^2 + (\dot{v}_j^l)^2 + (\dot{w}_j^l)^2] \Big|_{y=d_j} dx \end{aligned} \quad (3.3)$$

where n_i and n_j represent the number of circumferential and longitudinal stiffeners, ρ , ρ_c and ρ_l is the density of the cylindrical shell, circumferential and longitudinal stiffeners, respectively.

The stiffened cylindrical shell is simply supported at its two ends. The boundary conditions of the stiffened cylindrical shell at both ends are

$$\begin{aligned} v|_{x=0} = 0 & & w|_{x=0} = 0 & & N_x|_{x=0} = 0 & & M_x|_{x=0} = 0 \\ v|_{x=L} = 0 & & w|_{x=L} = 0 & & N_x|_{x=L} = 0 & & M_x|_{x=L} = 0 \end{aligned} \quad (3.4)$$

In order to satisfy the boundary conditions, Eqs. (3.3), the displacement functions of the laminated cylindrical shell are assumed as

$$\begin{aligned} u &= u_{mn} \sin(\omega_{mn}t) \cos \frac{m\pi x}{L} \sin \frac{ny}{R} & v &= v_{mn} \sin(\omega_{mn}t) \sin \frac{m\pi x}{L} \cos \frac{ny}{R} \\ w &= w_{mn} \sin(\omega_{mn}t) \sin \frac{m\pi x}{L} \sin \frac{ny}{R} \end{aligned} \quad (3.5)$$

where u_{mn} , v_{mn} and w_{mn} are undetermined coefficients, ω_{mn} is the natural angular frequency of the stiffened cylindrical shell, m and n represent the number of half waves in the axial and circumferential directions respectively, and t is time. Due to continuity conditions (2.4), it is assumed that the form of the displacement functions of the circumferential and longitudinal ribs is consistent with that of the cylindrical shell, i.e. u_i^c , v_i^c , w_i^c , u_j^l , v_j^l and w_j^l .

The cylindrical shell analyzed in this paper is symmetrically orthogonally laminated. Thus, the coupling effects of tension-shearing, tension-bending and bending-twisting in the cylindrical shell disappear. Substitute Eqs. (2.1)-(2.3) and (2.5)-(2.13) into Eqs. (3.2) and Eqs. (2.4) and (3.5) into Eqs. (3.3). By putting $B_{ij} = 0$, the strain energy and the kinetic energy of the stiffened composite cylindrical shell is derived

$$\begin{aligned} U &= \frac{\pi RL}{4} \left[D_{11} w_{mn}^2 \left(\frac{m\pi}{L} \right)^4 + 2D_{12} w_{mn}^2 \left(\frac{m\pi}{L} \right)^2 \left(\frac{n^2}{R^2} - \frac{1}{R^2} \right) + D_{22} w_{mn}^2 \left(\frac{n^2}{R^2} - \frac{1}{R^2} \right)^2 \right. \\ &+ 2D_{66} w_{mn}^2 \left(\frac{m\pi}{L} \right)^2 \left(\frac{n}{R} \right)^2 + A_{11} u_{mn}^2 \left(\frac{m\pi}{L} \right)^2 + 2A_{12} u_{mn} \frac{m\pi}{L} \left(\frac{nv_{mn}}{R} - \frac{w_{mn}}{R} \right) \\ &+ A_{22} \left(-\frac{nv_{mn}}{R} + \frac{w_{mn}}{R} \right)^2 + A_{66} \left(\frac{nu_{mn}}{R} + \frac{m\pi v_{mn}}{L} \right)^2 \left. \right] \\ &+ \sum_{i=0}^{n_i} \frac{b_c \pi R}{2} \left[A_{11}^{(c)} \left(-\frac{nv_{mn}}{R} + \frac{w_{mn}}{R} \right)^2 + D_{11}^{(c)} w_{mn}^2 \left(\frac{n}{R} \right)^4 \right. \\ &+ 2B_{11}^{(c)} \left(-\frac{nv_{mn}}{R} + \frac{w_{mn}}{R} \right) w_{mn} \left(\frac{n}{R} \right)^2 \left. \right] \sin^2 \frac{m\pi c_i}{L} \\ &+ \sum_{j=0}^{n_j} \frac{b_l L}{4} \left[A_{11}^{(l)} u_{mn}^2 \left(\frac{m\pi}{L} \right)^2 - 2B_{11}^{(l)} u_{mn} w_{mn} \left(\frac{m\pi}{L} \right)^3 + D_{11}^{(l)} w_{mn}^2 \left(\frac{m\pi}{L} \right)^4 \right] \sin^2 \frac{nd_j}{R} \end{aligned} \quad (3.6)$$

and

$$\begin{aligned} T &= \pi RL \rho h \omega_{mn}^2 (u_{mn}^2 + v_{mn}^2 + w_{mn}^2) \frac{\cos^2(\omega_{mn}t)}{4} \\ &+ \sum_{i=0}^{n_i} \rho_c b_c h_c \pi R \omega_{mn}^2 \left(u_{mn}^2 \cos^2 \frac{m\pi c_i}{L} + v_{mn}^2 \sin^2 \frac{m\pi c_i}{L} + w_{mn}^2 \sin^2 \frac{m\pi c_i}{L} \right) \frac{\cos^2(\omega_{mn}t)}{2} \\ &+ \sum_{j=0}^{n_j} \rho_l b_l h_l L \omega_{mn}^2 \left(u_{mn}^2 \sin^2 \frac{nd_j}{R} + v_{mn}^2 \cos^2 \frac{nd_j}{R} + w_{mn}^2 \sin^2 \frac{nd_j}{R} \right) \frac{\cos^2(\omega_{mn}t)}{4} \end{aligned} \quad (3.7)$$

The total potential energy Π of the stiffened cylindrical shell during free vibration is the superposition of the strain and kinetic energy, i.e.

$$\Pi = U + T \quad (3.8)$$

According to the principle of virtual work, the actual displacements u , v and w of the stiffened cylindrical shell during free vibration must be such that the first variation of the total potential energy per unit time is stationary. In particular, it must be a minimum under the condition of equilibrium. This condition is satisfied by taking the first derivative of the total potential energy per unit time \dot{I} with respect to u_{mn} , v_{mn} , w_{mn} , and set these values to zero, i.e.

$$\frac{\partial \dot{I}}{\partial u_{mn}} = 0 \quad \frac{\partial \dot{I}}{\partial v_{mn}} = 0 \quad \frac{\partial \dot{I}}{\partial w_{mn}} = 0 \quad (3.9)$$

From Eq. (3.9), a set of homogeneous linear equations about u_{mn} , v_{mn} and w_{mn} are obtained as follows

$$\begin{bmatrix} L_{11} & L_{12} & L_{13} \\ L_{21} & L_{22} & L_{23} \\ L_{31} & L_{32} & L_{33} \end{bmatrix} \begin{bmatrix} u_{mn} \\ v_{mn} \\ w_{mn} \end{bmatrix} = \mathbf{0} \quad (3.10)$$

The necessity for nontrivial solutions of Eq. (3.10) requires the determinant of the coefficient matrix $\mathbf{L}(\omega_{mn})$ to be zero

$$\begin{vmatrix} L_{11} & L_{12} & L_{13} \\ L_{21} & L_{22} & L_{23} \\ L_{31} & L_{32} & L_{33} \end{vmatrix} = 0 \quad (3.11)$$

where the coefficient L_{ij} is not only a function of ω_{mn} , but also in relation to the material properties and geometry parameters of the laminated cylindrical shell as well as the stiffeners. From Eq. (3.11), the natural frequency of the stiffened composite cylindrical shell is obtained through the MATLAB program and it can be converted into the natural frequency f_e by $\omega_{mn} = 2\pi f_e$.

4. Validation

In this Section, a simply supported cylindrical shell with 10 stiffeners in the circumferential and longitudinal direction is studied as an example to verify the validation of the energy method in Section 4. The laminated cylindrical shell is made of graphite/epoxy composite plies while the stiffeners are made of Q235 steel. The shell has a stacking sequence of $[0/90/0]_7$ with the thickness of 1 mm for each single composite ply. The geometric and material properties are given in Table 1. The natural frequency is calculated through the customized MATLAB program based on the energy method.

Table 1. Material properties and geometric parameters of stiffened cylindrical shell

Shell	Stiffeners	
	Circumferential	Longitudinal
$E_1 = 130 \text{ GPa}$, $E_2 = 9.5 \text{ GPa}$, $G_{12} = 6 \text{ GPa}$, $\mu_{12} = 0.3$, $L = 1.94 \text{ m}$, $R = 0.35 \text{ m}$, $h = 0.021 \text{ m}$, $t = 0.001 \text{ m}$, $\rho = 1210 \text{ kg/m}^3$	$E_c = 206 \text{ GPa}$, $\rho_c = 7900 \text{ kg/m}^3$, $b_c = 0.005 \text{ m}$, $h_c = 0.02 \text{ m}$	$E_l = 206 \text{ GPa}$, $\rho_l = 7900 \text{ kg/m}^3$, $b_l = 0.005 \text{ m}$, $h_l = 0.02 \text{ m}$

Numerical simulation of free vibration of the stiffened cylindrical shell is conducted by ABAQUS software. The geometric and material parameters in theoretical analysis are also used in the finite element model to ensure the comparability of analytical and numerical solutions. As shown in Fig. 3, the stiffened cylindrical shell is modeled by three parts: the shell,

circumferential and longitudinal stiffeners. Each part is discretized into a mesh with 4-node general-purpose shell elements, characterized as reduced integration with hourglass control and finite membrane strains. For the shell, the mesh consists of 60 elements around the circumference and 53 parts along the length; for the stiffeners, the element size is chosen as 0.5 mm in both the circumferential and radial direction. The three parts are assembled by tied constraints to form a monolithic stiffened cylindrical shell. At the two ends of the shell, the degrees of freedom in the circumferential and radial direction at each point are constrained to provide the simply supported boundary condition. The frequency step is built to achieve the free vibration analysis and obtain the eigenvalues f_{FEM} for comparison with the energy method.

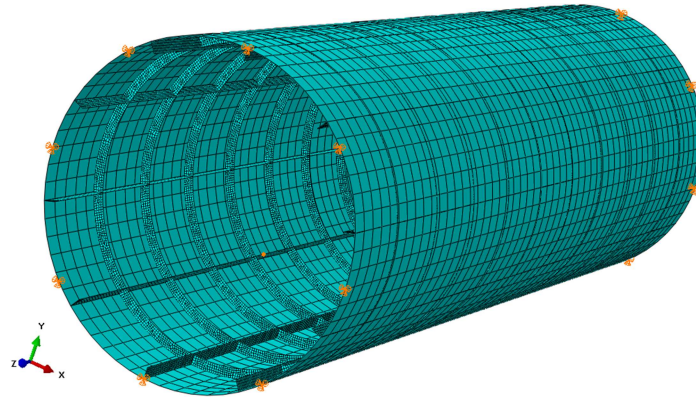


Fig. 3. Finite element model of the stiffened cylindrical shell

As illustrated in Fig. 4, the combination of various half-wave numbers in the circumferential and longitudinal directions forms different vibration modes of the stiffened cylindrical shell, which is consistent with the mode function assumed as in Eq. (3.5). The comparisons between analytical and numerical solutions are listed in Table 2. It can be seen that the solutions from the energy method f_e are in good agreement with those from the finite element analysis f_{FEM} , which indicates that the algorithm based on the energy method is accurate for predicting the free vibration characteristics of the stiffened cylindrical shell.

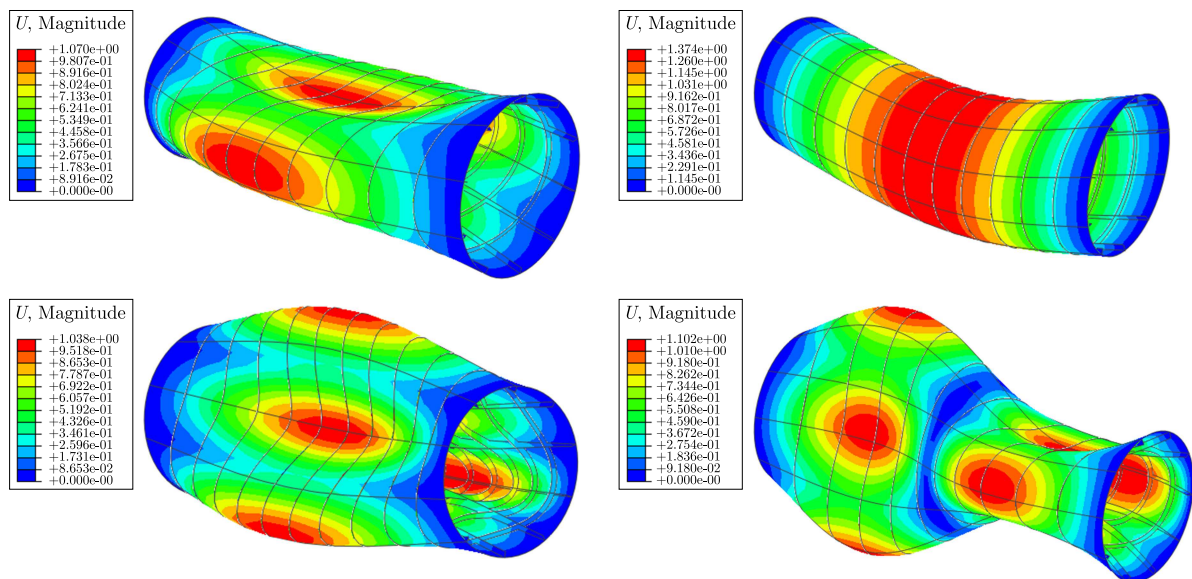


Fig. 4. Vibration modes of the finite element model of the stiffened cylindrical shell: (a) first order vibration mode ($m = 1, n = 2$), (b) second order vibration mode ($m = 1, n = 1$), (c) third order vibration mode ($m = 1, n = 3$), (d) fourth order vibration mode ($m = 2, n = 2$)

Table 2. Comparisons of the first to sixth order natural frequencies of stiffened cylindrical shells

m	n	f_e [Hz]	f_{FEM} [Hz]	Error [%]
1	2	234.88	249.58	6.26
1	1	322.43	341.85	6.02
1	3	432.34	417.15	3.51
2	2	442.44	437.19	1.16
2	3	512.45	491.62	4.06
3	3	636.54	619.48	2.68

5. Parameter analysis and stiffener optimization

The validation of theoretical solution as well as finite element model has been demonstrated in the foregoing Section by comparing both with each other. In this Section, a parametric study is conducted using the established energy method and finite element model to illustrate the influence of different numbers, geometric parameters and material properties of the stiffeners on the free vibration of the stiffened cylindrical shell.

5.1. The influence of numbers of stiffeners

Figure 5 illustrates the influence of numbers of stiffeners on the first order natural frequency f_1 of the stiffened cylindrical shell reinforced in only the circumferential or longitudinal direction. Cases in which $n_i = n_j = 0, 10, 20, 30, 40$ and 50 are investigated. In addition,

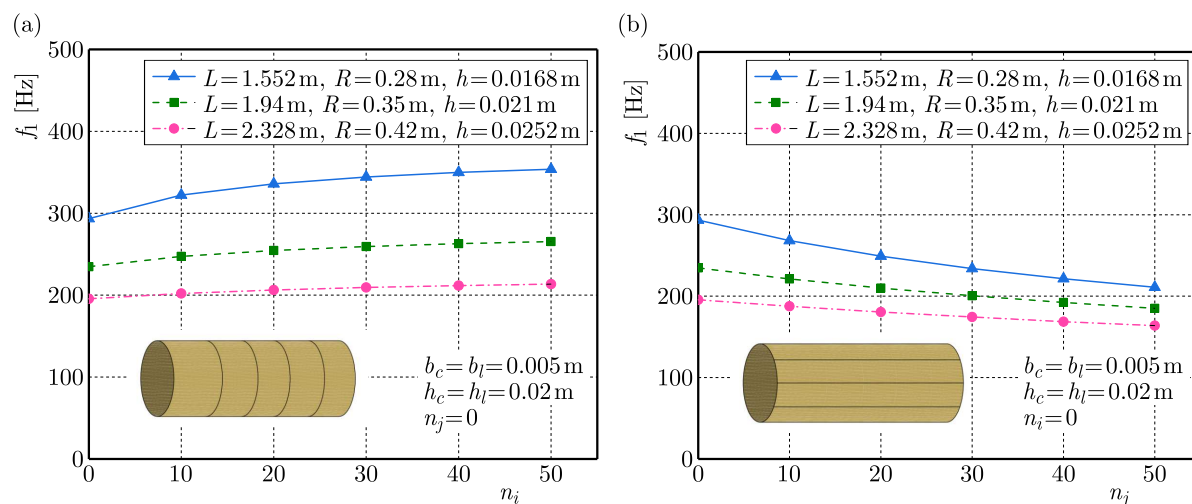


Fig. 5. Curves of the first order natural frequency of the stiffened cylindrical shell varying with the number of stiffeners: (a) circumferential stiffeners, (b) longitudinal stiffeners

variations of frequencies with respect to different geometric parameters but the same radius-to-thickness ratio R/h and length-to-radius ratio L/R are observed by changing the radius R , length L and thickness h of the shell. It can be seen from the curves that in the case of different geometric parameters of the shell, as the number of circumferential stiffeners n_i rises, the first order natural frequency f_1 always enlarges. However, the frequencies decrease with an increase in the number of longitudinal stiffeners, which results from the difference in the contribution of longitudinal stiffeners to the strain and kinetic energy of the structure. For the free vibration of the shell, circumferential bending is the dominant deformation, but the effect of longitudinal

stiffeners on the circumferential bending is negligible. Therefore, the kinetic energy of the structure increases obviously while the variation of strain energy can be ignored, which results in the reduction of the natural frequency.

5.2. The influence of geometric parameters of stiffeners

The influence of geometric parameters of stiffeners on the free vibration performance is shown in Fig. 6. Analyses are conducted for the cases of $b_c = b_l = 0.005$ m, 0.01 m, 0.015 m, 0.02 m, 0.025 m and $h_c = h_l = 0.02$ m, 0.04 m, 0.06 m, 0.08 m, 0.1 m, in which the area increments of the stiffeners in the parameter analysis are controlled the same.

As shown in Fig. 6, the first order natural frequency f_1 increases with the increment of geometric parameters of the circumferential stiffeners, including the width b_c and height h_c . In addition, comparing the curves of the circumferential stiffeners in Figs. 6a and 6b, it can be found that when the area increment is given, the increasing of the height of the stiffener has a greater impact on the frequency than the width. This is because D_{11c} has a cubic term of h_c in the calculation of the strain energy, whereas b_c only exists in the form of a first term. Thus, h_c plays a major role in the energy conversion process, which indicates that the free vibration of the stiffened shell is behavior dominated by circumferential bending. However, it can be found in Fig. 6 that the frequency f_1 decreases with an increase in the width b_l or height h_l , which can also be attributed to the the difference between the strain energy and the kinetic energy caused by the longitudinal stiffeners.

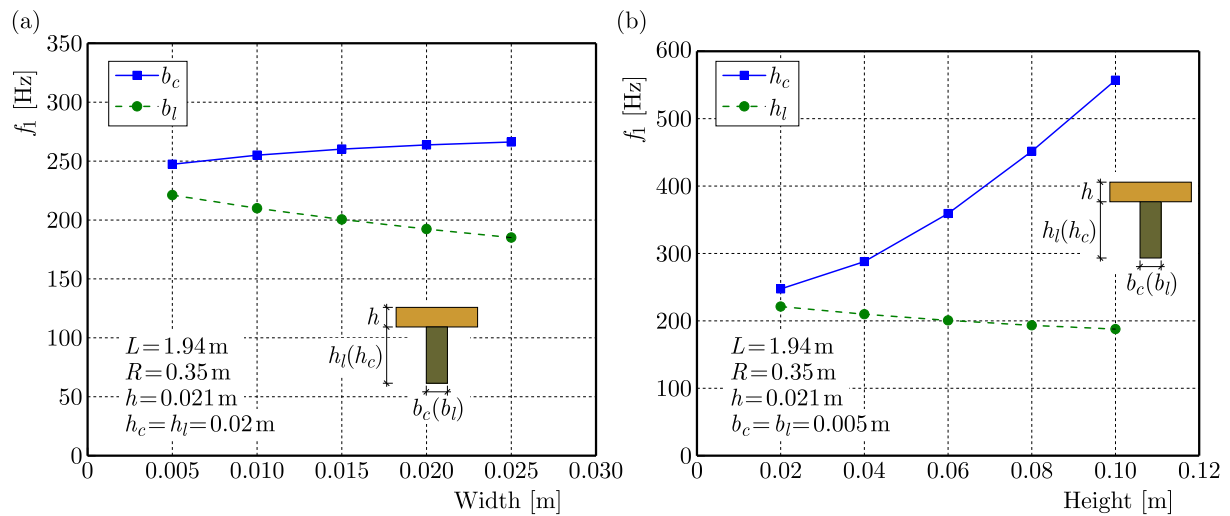


Fig. 6. Curves of the first order natural frequency of stiffened cylindrical shell varying with geometric parameters of stiffeners: (a) width, (b) height

5.3. The influence of material properties of stiffeners

Figure 7 is a schematic diagram of the influence of Young's modulus E_r and E_s on the first order natural frequency f_1 for materials with the same physical and geometric properties but different E_c and E_l . As illustrated in Fig. 7a, although the frequency f_1 increases obviously with the increase in Young's modulus E_c , the frequency f_1 is almost insusceptible to the variation of E_l . The reason for this phenomenon is that the strain energy is directly related to the elastic modulus, but the increase in longitudinal stiffness of the structure caused by the increase of E_l has negligible influence on the free vibration of the cylindrical shell dominated by bending in the circumferential direction.

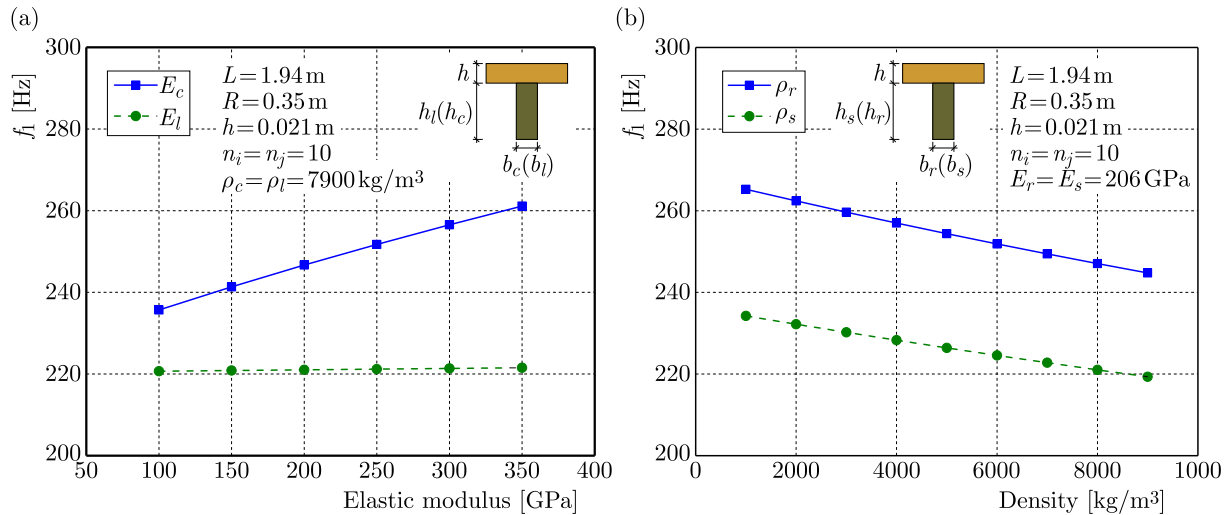


Fig. 7. Curves of the first order natural frequency of stiffened cylindrical shell varying with material properties of stiffeners: (a) elastic modulus, (b) density

The variation of the first order natural frequency f_1 with the density ρ_c and ρ_l of the stiffeners is plotted in Fig. 7b. As shown in Fig. 7b, when the density increases from 1000 kg/m³ to 9000 kg/m³, the frequency of the shell structure shows a decline in both circumferential or longitudinal reinforcement schemes. Comparing the slopes of the two curves, it can be found that the change of the elastic modulus has a slightly greater effect on the natural frequency of the circumferential reinforced cylindrical shell than that stiffened in the longitudinal direction.

5.4. Optimization of the reinforcement scheme

According to the above analysis, it can be concluded that for the free vibration of the stiffened cylindrical shell, the circumferential stiffener plays a major role in the influence on the natural frequency of the structure, whereas the effect of the longitudinal stiffeners on the natural frequency of the structure is negligible. Therefore, during the design of a stiffened cylindrical shell, the circumferential stiffeners should take precedence over longitudinal stiffeners to improve vibration characteristics of the structure. In addition, in the determination of the geometric parameters of the stiffeners, priority should be given to the increase in the height of circumferential stiffeners for a higher efficiency in improving the frequency of the structure. For the material properties of stiffeners, a high elastic modulus and low density are of great significance to the free vibration of the stiffened cylindrical shell.

6. Conclusion

In the present study, the problems of free vibration of the stiffened cylindrical shell was investigated by means of theoretical analysis and numerical simulation. Based on the Kármán-Donnell's shell theory and the principle of minimum potential energy, the strain and kinetic energy of the shell and stiffeners were calculated and the matrix $\mathbf{L}(\omega_{mm})$ relation to the frequency was established. Furthermore, finite element models were built to verify the validation of analytical solutions, and a good agreement was found in the comparison between the theoretical and numerical solutions. To explore the stiffening optimization of the cylindrical shell, parametric studies were performed to ascertain the influences of numbers, geometric parameters and material properties of the stiffeners on the natural frequency of the stiffened cylindrical shell. The following conclusions can be drawn:

- The free vibration mode of the stiffened cylindrical shell is still dominated by the shell, showing a half-wave distribution in the circumferential and longitudinal directions. Moreover, as the vibration modal order increases, the half-wave number in the circumferential and longitudinal directions gradually increases.
- The free vibration of the stiffened cylindrical shell is dominated by the circumferential bending behavior. The installation of circumferential stiffeners has a significant effect on the frequency increase while the reinforcement in the longitudinal direction results in the reduction of the frequency. It is found that when the number of the stiffeners exceeds 10, the frequency of the cylindrical shell increases very slowly.
- The geometric parameters of the stiffeners play an important role on the free vibration of the stiffened cylindrical shell. The variation trend of the frequency of the stiffened cylindrical shell caused by a change in width or height of the stiffeners is consistent with the trend resulted from the variation of number of stiffeners. Furthermore, the change of height has a more significant influence on the frequency than the width.
- An increase in the elastic modulus of stiffeners leads to a rise of strain energy of the stiffened cylindrical shell, which causes an increase in the frequency. In contrast, an increase in density results in a rise of kinetic energy of the structure, which causes reduction of the frequency. Following this observation, it is better to choose rolled steels with a high elastic modulus as the stiffeners, for instance, bearing steel with high Chromium, since the density of various steels changes quite little.

Acknowledgment

The work presented herein was conducted with the financial support of Natural Science Foundation of Guangdong Province (2021A1515012037).

References

1. AHMADI H., FOROUTAN K., 2019, Nonlinear vibration of stiffened multilayer FG cylindrical shells with spiral stiffeners rested on damping and elastic foundation in thermal environment, *Thin-Walled Structures*, **145**, 106388
2. BISAGNI C., CORDISCO P., 2006, Post-buckling and collapse experiments of stiffened composite cylindrical shells subjected to axial loading and torque, *Composite Structures*, **73**, 138-149
3. BRESLAVSKII I.D., STREL'NIKOVA E.A., AVRAMOV K.V., 2011, Free vibrations of a shallow shell in fluid under geometrically nonlinear deformation, *Strength of Materials*, **43**, 1, 25-32
4. GAN L., LI X.B., ZHANG Z., 2009, Free vibration analysis of ring-stiffened cylindrical shells using wave propagation approach, *Journal of Sound and Vibration*, **326**, 633-646
5. HEMMATNEZHAD M., RAHIMI G.H., TAJIK M., PELLICANO F., 2015, Experimental, numerical and analytical investigation of free vibrational behavior of GFRP-stiffened composite cylindrical shells, *Composite Structures*, **120**, 509-518
6. JAFARI A. A., BAGHERI M., 2006, Free vibration of non-uniformly ring stiffened cylindrical shells using analytical, experimental and numerical methods, *Thin-Walled Structures*, **44**, 82-90
7. LEE H.W., KWAK M.K., 2015, Free vibration analysis of a circular cylindrical shell using the Rayleigh-Ritz method and comparison of different shell theories, *Journal of Sound and Vibration*, **353**, 344-377
8. LI Y.K., SUN W.H., DUAN G., LIANG J.H., 2013, Stress calculation for large storage oil tanks' shells based on the theory of short cylindrical shell, *Advanced Material Research*, **602-604**, 2163-2169
9. LI Z.L., HU H., YU W., 2015, Free vibration of joined and orthogonally stiffened cylindrical-spherical shells, *Journal of Vibration and Shock*, **34**, 22, 129-137

10. MOHAMAD S.Q., 2002, Recent research advances in the dynamic behavior of shells: 1989-2000, Part 1: Laminated composite shells, *Applied Mechanics Reviews*, **55**, 4, 325-350
11. MOHAMAD S.Q., SULLIVAN R.W., WANG W., 2010, Recent research advances on the dynamic analysis of composite shells: 2000-2009, *Composite Structures*, **93**, 14-31
12. QIN Z.Y., PANG X.J., SAFAEI B., CHU F.L., 2019, Free vibration analysis of rotating functionally graded CNT reinforced composite cylindrical shells with arbitrary boundary conditions, *Composite Structures*, **220**, 847-860
13. ROUT M., BANDYOPADHYAY T., KARMAKAR A., 2017, Free vibration analysis of pretwisted delaminated composite stiffened shallow shells: A finite element approach, *Journal of Reinforced Plastics and Composites*, **36**, 8, 619-636
14. SADEGHIFAR M., BAGHERI M., JAFARI A.A., 2010, Multiobjective optimization of orthogonally stiffened cylindrical shells for minimum weight and maximum axial buckling load, *Thin-Walled Structures*, **48**, 12, 979-988
15. SADOVSKÝ Z., ĎURICOVÁ A., IVANČO V., KRIVÁČEK J., 2009, Imperfection measures of eigen- and periodic modes of axially loaded stringer-stiffened cylindrical shell, *Proceedings of the Institution of Mechanical Engineers, Part G – Journal of Aerospace Engineering*, **224**, 601-612
16. SCHNEIDER W., ZAHLTEN W., 2004, Load-bearing behaviour and structural analysis of slender ring-stiffened cylindrical shells under quasi-static wind load, *Journal of Constructional Steel Research*, **60**, 125-146
17. SHENG G.G., WANG, X., 2018, The dynamic stability and nonlinear vibration analysis of stiffened functionally graded cylindrical shells, *Applied Mathematical Modelling*, **56**, 389-403
18. SWAMY NAIDU N.V., SINHA P.K., 2007, Nonlinear free vibration analysis of laminated composite shells in hygrothermal environments, *Composite Structures*, **77**, 475-483
19. TORKAMANI SH., NAVAZI H.M., JAFARI A.A., BAGHERI M., 2009, 2009, Structural similitude in free vibration of orthogonally stiffened cylindrical shells, *Thin-Walled Structures*, **47**, 1316-1330
20. WANG X.T., YAO W., LIANG C., JI N., 2007, Stability characteristics of ring-stiffened cylindrical shells under different longitudinal and transverse external pressures, *Journal of Marine Science and Application*, **6**, 3, 33-38
21. XUE J.H., 2012, Local buckling in infinitely, long cylindrical shells subjected uniform external pressure, *Thin-Walled Structures*, **53**, 211-216
22. XUE J.H., 2013, Post-buckling analysis of the length of transition zone in a buckle propagating pipeline, *Journal of Applied Mechanics*, **80**, 5, 051002
23. XUE J.H., WANG Y., YUAN D., 2015, A shear deformation theory for bending and buckling of undersea sandwich pipes, *Composite Structures*, **132**, 633-643
24. XUE J.H., YUAN D., HAN F., LIU R., 2013, An extension of Kármán-Donnell's theory for non-shallow, long cylindrical shells undergoing large deflection, *European Journal of Mechanics A/Solids*, **37**, 329-335
25. ZHOU X.P., 2012, Vibration and stability of ring-stiffened thin-walled cylindrical shells conveying fluid, *Acta Mechanica Sinica*, **25**, 2, 168-176